

Figure 1. Schematic illustration of the model. The particles (represented as circles) are hard disks of finite area moving at fixed speed in the periodic domain (the dashed greyed-out particle is re-inserted at its periodic location). Their ballistic trajectories are interrupted by momentum-conserving collisions (blue semi-filled circles). New particles (red filled circle) are inserted at random non-occupied positions, with velocity given by the corresponding thermal distribution, and at times prescribed by the growth kinetics.

where  $n(t)$  is the number of particles per unit area at time  $t$ . Growth of the population is envisioned as the arrival of randomly spaced particles according to a predetermined growth curve which – in keeping with the model of a cell population in culture – we take to be the logistic curve

$$n(t) = \frac{kn_0 e^{\rho t}}{k + n_0(e^{\rho t} - 1)}, \quad (2)$$

with  $n_0$  and  $k$  respectively the initial and the maximal particle densities and  $\rho$  the rate of growth. We limit ourselves to a confluency  $c(t) \ll 1$ , effectively considering a dilute regime for the collisional dynamics. This limitation is also necessary to make sure that new particles can be inserted easily in the system.

### Diffusion coefficient for dilute hard disks

To estimate the motility at a given particle density  $n$  we compute the velocity autocorrelation function (VACF) of a single test particle:

$$\langle \mathbf{v}(t) \cdot \mathbf{v}(t + \tau) \rangle = \langle \cos \theta(\tau) s(t)s(t + \tau) \rangle, \quad (3)$$

where  $\mathbf{v}$  is the 2D velocity of a particle, the brackets indicate ensemble averaging,  $s$  is the norm of the particle's velocity vector (the particle speed),  $\theta(\tau)$  is the angle between its velocities at  $t$  and  $t + \tau$ , and  $\cdot$  is the scalar product. If the particle moves undisturbed in the short time  $\tau$ , then  $\theta(\tau) = 0$ ,  $s(t + \tau) = s(t)$ , and thus  $\mathbf{v}(t) \cdot \mathbf{v}(t + \tau) = s(t)^2$ . If on the other hand the particle undergoes a collision in this time, the autocorrelation will depend on the form of the interaction. Assuming isotropic interactions, there will be a class of

systems for which  $\theta(\tau)$  can be modelled as a random uniformly distributed angle independent of the particle speed, such that the many particle average  $\langle \cos \theta(\tau) \rangle$  and thus  $\langle \mathbf{v}(t) \cdot \mathbf{v}(t + \tau) \rangle_{\text{coll}}$  vanishes. Then for a large ensemble only those particles which have not yet collided will contribute to the VACF. For a system in thermal equilibrium the occurrence of collisions may reasonably be modelled as a memoryless stochastic process, so that the inter-collision time is given by the exponential distribution:  $\mathbb{P}\{\text{no collision in } \tau\} = e^{-\lambda\tau}$  with  $1/\lambda$  the average inter-collision time. The VACF is thus

$$\langle \mathbf{v}(t) \cdot \mathbf{v}(t + \tau) \rangle = \langle s(t)^2 \rangle e^{-\lambda|\tau|}. \quad (4)$$

By integrating Eq. (4), we obtain through the Green-Kubo relation (see for instance the Ornstein-Uhlenbeck example in Ref. [15]) the spatial diffusion coefficient

$$\mathcal{D} = \frac{1}{2} \int_0^\infty \langle \mathbf{v}(t) \cdot \mathbf{v}(t + \tau) \rangle d\tau = \frac{\langle s(t)^2 \rangle}{2\lambda} \quad (5)$$

(where the factor 1/2 comes from the fact that we work in two spatial dimensions), so that in absence of growth we expect a linear mean squared displacement (MSD) in equilibrium:  $\langle \mathbf{x}(t)^2 \rangle = 4\mathcal{D}t$ .

### Effective Langevin dynamics

We establish here the link between the diffusion coefficient computed in the previous section and the Langevin equation (LE) in two dimensions:

$$\frac{d\mathbf{v}(t)}{dt} = -\gamma\mathbf{v}(t) + \sqrt{2\eta}\xi(t), \quad (6)$$

where  $\xi(t)$  is white noise [15]:

$$\langle \xi(t) \rangle = 0 \quad \text{and} \quad \langle \xi_i(t)\xi_j(t') \rangle = \delta(t - t')\delta_{i,j}, \quad (7)$$

$\gamma$  is the friction coefficient and  $\eta$  is the noise intensity. Integration of Eq. (6) provides the autocorrelation function

$$\langle \mathbf{v}(t) \cdot \mathbf{v}(t + \tau) \rangle = \frac{2\eta}{\gamma} e^{-\gamma|\tau|}. \quad (8)$$

For  $\tau = 0$  we find the second moment of the speed

$$\langle s(t)^2 \rangle = 2\eta/\gamma. \quad (9)$$

Inserting this back into Eq. (8) and comparing with Eq. (4), we see that the autocorrelation functions for the Brownian particle and the ensemble of interacting particles are in fact equal upon identification of  $\lambda = \gamma$ . We use this correspondence to interpret the Langevin dynamics of Eq. (6) as an averaged description of the particle paths in the interacting ensemble, with the expected time between collisions encoded in the Brownian friction coefficient as  $1/\gamma$ . For the simple dynamical model of hard

disks, we can now estimate the friction and noise intensity directly from the physical parameters so that – in equilibrium – we can use Eq. (6) without fitting any parameter. In the dilute regime, we can express the mean inter-collision time as a function of the mean free path  $l$ , which in turn can be coupled to the particle density  $n$  (with  $\sigma = 2d$  the collisional cross section) [16]:

$$l = \frac{\langle s \rangle}{\gamma} = 1/\sqrt{2}\sigma n . \quad (10)$$

At equilibrium, the speed distribution can be shown to approach the Rayleigh distribution [4] with mean

$$\langle s \rangle = \sqrt{\eta\pi/2\gamma} , \quad (11)$$

and the fluctuation-dissipation relation dictates the relation between  $\gamma$  and  $\eta$

$$k_B T = \eta/\gamma . \quad (12)$$

Thus combining Eqs. (10), (11), and (12), we may write the coefficients in the Langevin equation in terms of the particle density and system temperature:

$$\begin{cases} \gamma = \sqrt{\pi k_B T} \sigma n \\ \eta = k_B T \gamma \end{cases} \quad (13)$$

Using the derivations above and Eqs. (5) and (9), we obtain the spatial diffusion coefficient

$$\mathcal{D} = \eta/\gamma^2 = \sqrt{k_B T/\pi} (\sigma n)^{-1} . \quad (14)$$

Up to this point we have silently assumed that the particle density of the system is constant, both in the derivation of the velocity autocorrelation as well as in the assumption of an equilibrium speed distribution. It is however worth investigating to what extent Eq. (13) holds if the particle density varies slowly. For example, we might envision a population of cells undergoing divisions, where the growth rate is slow enough that many collisions occur in between mitotic events. If then the equilibrium assumption remains adequate, the LE in Eq. (6) can be used with time-dependent coefficients  $\gamma(t)$  and  $\eta(t)$  to obtain statistical properties of the particles subject to the growth function  $n(t)$ .

While solving the LE with time-dependent coefficients is difficult, we can also investigate the validity of an overdamped approximation, which corresponds to taking  $d\mathbf{v}(t)/dt = 0$ . This permits a straightforward solution of the LE, as the corresponding Fokker-Planck equation is simply the diffusion equation with time dependent diffusion coefficient Eq. (14). This can be solved in the usual manner and results in the MSD

$$\langle \mathbf{x}(t)^2 \rangle = 4 \int_0^t \mathcal{D}(t') dt' . \quad (15)$$

## Simulations

To test the validity of this approach we also study the hard disk system with event-driven simulations. We place the disks in a periodic domain and assign random initial velocities such that the average kinetic energy per particle is  $k_B T$ . Due to the randomness of the initial velocity distribution the system will generally present a nonzero center-of-mass drift, which we remove before initiating dynamics. The simulation then proceeds in an event-driven manner. At the start of each increment, all particles are moved according to their current velocity. Next, potential collisions (detected as overlapping surfaces) are identified and sorted in order of occurrence. Collisions are then performed successively – with newly occurring overlaps being similarly detected, timed, and added to the queue – until all overlaps have been treated. Population growth is implemented by the introduction of new particles at random positions in the simulation area and fixed times according to the growth curve in Eq. (2). Newly birthed particles are added with initial speed  $\sqrt{2k_B T}$  to ensure the system evolves isothermally [17]. To compare simulation results of the density-varying system with the Langevin model (13) we compute stochastic realizations of the equation with the SOSRI algorithm [18] using the Julia package DifferentialEquations.jl [19].

## MODEL RESULTS

For systems where the particle density remains fixed, we find the accuracy of the Langevin model to depend on the confluency. The predicted diffusion coefficient agrees well with simulations of the hard-disk particle dynamics for  $c \leq 0.1$ , whereas for higher particle densities the error grows as the available volume is increasingly occupied (Figure 2). The origin of this error can be found in our assumption of independent collisions with a well defined mean free path (10), which gives a poor representation of the hard-disk system when its value approaches the order of the collisional cross section. In the low density limit the model's validity is principally restricted by the timescale of interest, since if the characteristic collision time  $1/\gamma$  is larger than the timescale the individual particle motion is effectively ballistic and Brownian motion does not apply. However for a large number of particles the ensemble statistics remained in agreement even for the lowest density investigated ( $c = 0.01$ ) at a timescale of a hundredth of the characteristic time.

When population growth is introduced the particle density increases and the Langevin parameters  $\gamma$  and  $\eta$  are no longer constant in time. We investigate the validity of the density-dependent model with respect to the hard-disk system under isothermal growth by simulating the addition of particles at randomly distributed posi-

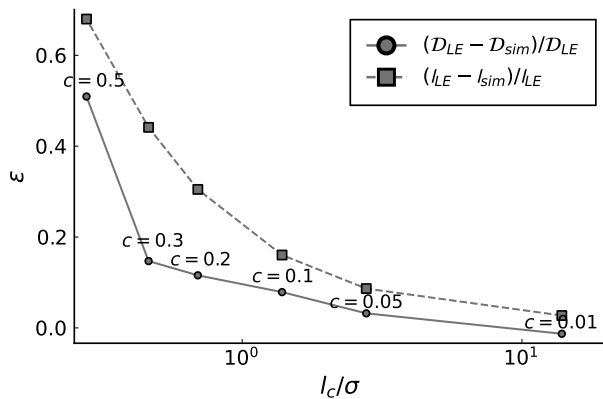


Figure 2. The relative errors on the diffusion coefficient  $D$  predicted by Eq. (14) and the mean inter-collision distance  $l$  predicted by Eq. (10) with respect to simulations at fixed density, as a function of the ratio of the inter-collision distance to the collisional cross section. The simulations consisted of 2000 individual particles for each confluency investigated.

tions at a rate prescribed by the growth function. As an illustrative example we consider the case of logistic growth (2) for different rate parameters  $\rho$ , shown in Figure 3a. We observe that as the density rises the inter-collision time decreases, resulting in a decreasing variation of the particle MSD during the growth period and thus apparent subdiffusive motion (Figure 3b-d). Once the maximal population density is reached the slope of the MSD becomes constant. Such a linear limit of the functional form of the MSD for large times is an indicator of classical diffusion (Figure 3c-d).

As intended, simulations of the LE show good agreement with the particle simulations in the quasi-equilibrium parameter regime (Figure 3c), where the rate of growth is smaller than the time between collisions. Furthermore, the overdamped approximation of Eq. (15) agrees well with the subdiffusive variation of the MSD, however, as to be expected it does not capture the initial short time ballistic motion (Figure 3b), resulting in an eventual overestimation of the displacement (Figure 3c). Interestingly, the LE model maintains similar accuracy even if the growth rate is significantly higher, as a growth rate of up to 25 times the inter-collision time was tested.

## DISCUSSION

We have shown how a 2D system of ballistic hard-disk particles subject to population level density dynamics can be modeled by an effective Brownian Langevin equation, in which the friction  $\gamma$  and force intensity  $\eta$  are made to depend explicitly on the particle density of the system. This parameter-free dependence is obtained by employing a classic model for the mean inter-collision

distance that – with the assumption of memoryless collisions – arises in the velocity autocorrelation function of the LE. By comparison with simulations of the system, we showed the model to be accurate up to a confluency of around 0.1. For higher densities we found the error on the mean inter-collision distance to grow rapidly with confluency, implying that the LE could potentially remain accurate under a different model for the free path lengths.

To test the validity of the LE in the case of a dynamically varying density – where the assumption of thermal equilibrium is in principle no longer valid – we investigated a model system where new particles are added according to a logistic growth function. The mean-squared displacement under these conditions becomes non-linear, reflecting the changing dynamic parameters. Comparing statistics from numerical simulations of the density dependent LE with the particle simulations showed agreement up to the highest growth rates investigated. The good correspondence at such growth rates comes as a surprise, considering the equilibrium assumptions used to derive the LE. We can think of a number reasons why this is the case, such as the fact that we insert particles from a thermal distribution at random locations, thus not promoting spatial inhomogeneity, and the dilute nature of the gas. However, we have no formal explanation to elucidate this matter.

While the specific system studied here may appear restrictive, it is illustrative of the potential for modeling the effect of stochastically occurring interactions within a density-varying population as an effective random walk. A generalization to three spatial dimensions would be straightforward, the main difference in the derivation being that the Maxwell-Boltzmann distribution must be taken for the particle speeds. Furthermore, the inclusion of external forces can be achieved by introducing their relevant potentials in the LE. The consideration of more complicated interaction effects – such as for example aligning forces [8] or particle-generated flow fields in a background fluid [20] – likely presents a greater challenge, as the method described here exploits a simple statistical uniformity of interactions – i.e. the particle’s direction of motion following a collision modeled as a uniform distribution. Nevertheless, such interactions can in principle be included through multi-particle potentials in the LE, for which various analysis procedures exist in the literature (see for example [6], [20] or [7]). Finally, the application of the LE derived here need not be constrained to the case of ballistically moving particles, as it can simply be added to the LE of more complex motions, serving as a population effect on the movement of individual particles. With growing interest in biological systems where proliferation is present, this approach provides a useful alternative to modeling interactions directly.

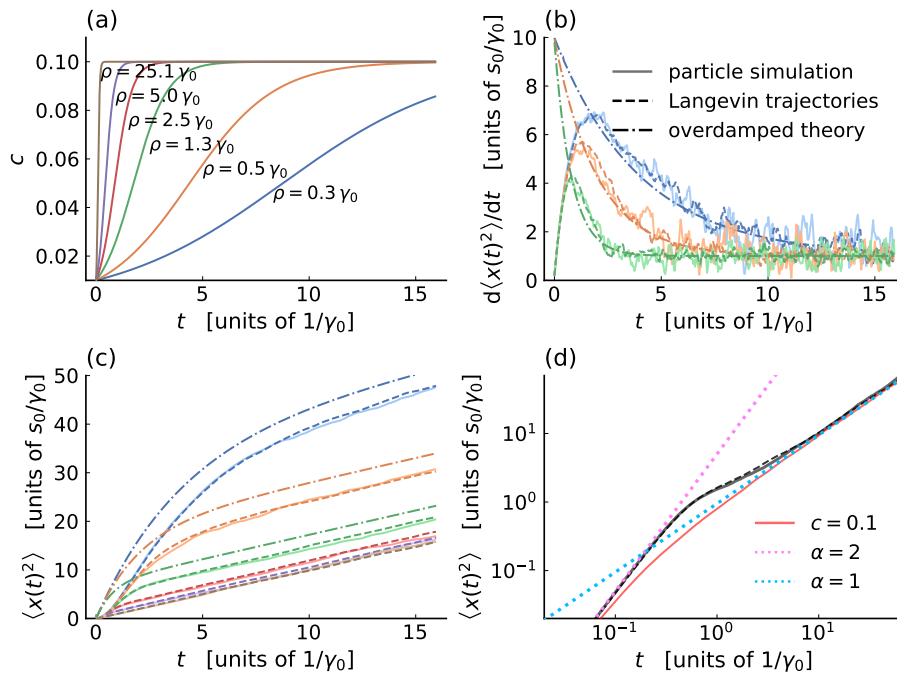


Figure 3. Dynamics of particles in populations with density subject to the logistic growth function (2). Results for different growth rates  $\rho$  are shown in populations with initial confluency  $c = 0.01$  (1000 particles) and maximal capacity  $c = 0.1$  (10'000 particles). Time and distance are presented in units of the average inter-collision time for the initial density  $1/\gamma_0$  and the average inter-collision distance  $s_0/\gamma_0$ . (a) Confluency over time. (b) Derivative of the MSD obtained from particle simulations (solid lines), simulations of the LE (dashed lines), and predicted by the overdamped approximation (dash-dotted lines), for the slowest growth rates used in (a), increasing from top to bottom. (c) MSD under all simulated growth rates for particle simulations (same legend as (b); for clarity, the overdamped prediction is not shown for the highest growth rates). (d) Log-log plot of the MSD under growth rate  $\rho = 5.0\gamma_0$ , compared to a simulation at fixed confluency  $c = 0.1$  (solid red line). Additional trendlines (dotted)  $f_\alpha(t) \propto t^\alpha$  are shown to illustrate motion type:  $\alpha = 1$  adheres to classical diffusion, whereas  $\alpha = 2$  implies ballistic motion.

\* Correspondence to: n.monpere@qmul.ac.uk

† These authors contributed equally.

- [1] K. Pearson and J. Blakeman, *A mathematical theory of random migration*, Vol. 15 (Dulau and Company, 1906).
- [2] H. C. Berg, *Random Walks in Biology* (Princeton University Press, 1983).
- [3] M. E. Cates, Diffusive transport without detailed balance in motile bacteria: does microbiology need statistical physics?, *Reports on Progress in Physics* **75**, 042601 (2012).
- [4] P. Romanczuk, M. Bär, W. Ebeling, B. Lindner, and L. Schimansky-Geier, Active brownian particles, *The European Physical Journal Special Topics* **202**, 1 (2012).
- [5] Y. Fily and M. C. Marchetti, Athermal phase separation of self-propelled particles with no alignment, *Physical Review Letters* **108**, 235702 (2012).
- [6] J. Tailleur and M. E. Cates, Statistical mechanics of interacting run-and-tumble bacteria, *Physical Review Letters* **100**, 218103 (2008).
- [7] J. Stenhammar, A. Tiribocchi, R. J. Allen, D. Marenduzzo, and M. E. Cates, Continuum theory of phase separation kinetics for active brownian particles, *Physical Review Letters* **111**, 145702 (2013).
- [8] T. Vicsek, A. Czirók, E. Ben-Jacob, I. Cohen, and O. Shochet, Novel type of phase transition in a system of self-driven particles, *Physical review letters* **75**, 1226 (1995).
- [9] M. Lintz, A. Muñoz, and C. A. Reinhart-King, The mechanics of single cell and collective migration of tumor cells, *Journal of Biomechanical Engineering* **139**, 10.1115/1.4035121 (2017), publisher: American Society of Mechanical Engineers Digital Collection.
- [10] P.-H. Wu, D. M. Gilkes, and D. Wirtz, The biophysics of 3d cell migration, *Annual Review of Biophysics* **47**, 549 (2018).
- [11] C. J. Weijer, Collective cell migration in development, *Journal of Cell Science* **122**, 3215 (2009).
- [12] P. Friedl and D. Gilmour, Collective cell migration in morphogenesis, regeneration and cancer, *Nature Reviews Molecular Cell Biology* **10**, 445 (2009), number: 7 Publisher: Nature Publishing Group.
- [13] W. Risau, Mechanisms of angiogenesis, *Nature* **386**, 671 (1997), number: 6626 Publisher: Nature Publishing Group.
- [14] K.-C. Lin, G. Torga, Y. Sun, R. Axelrod, K. J. Pienta, J. C. Sturm, and R. H. Austin, The role of heterogeneous environment and docetaxel gradient in the emergence of polyploid, mesenchymal and resistant prostate cancer cells, *Clinical & Experimental Metastasis* **36**, 97

- (2019).
- [15] C. W. Gardiner, *Handbook of stochastic methods for physics, chemistry, and the natural sciences*, 3rd ed., Springer series in synergetics (Springer, 2004).
- [16] S. Chapman and T. G. Cowling, *The mathematical theory of non-uniform gases: an account of the kinetic theory of viscosity, thermal conduction and diffusion in gases*, 3rd ed. (Cambridge university press, 1990) pp. 87–88.
- [17] The simulation code, written with the Julia programming language, is available at <https://github.com/natevmp/particle-crowding>.
- [18] C. Rackauckas and Q. Nie, Stability-optimized high order methods and stiffness detection for pathwise stiff stochastic differential equations, in *2020 IEEE High Performance Extreme Computing Conference (HPEC)* (IEEE, 2020) pp. 1–8.
- [19] C. Rackauckas and Q. Nie, Differentialequations.jl—a performant and feature-rich ecosystem for solving differential equations in julia, *Journal of Open Research Software* **5** (2017).
- [20] A. Baskaran and M. C. Marchetti, Statistical mechanics and hydrodynamics of bacterial suspensions, *Proceedings of the National Academy of Sciences* **106**, 15567 (2009).